AWES2020
20th Australasian Wind Engineering Society Workshop
8 – 9 April, 2021

Building porosity and its influence on internal pressure

M.T Humphreys[1], J. D. Ginger[2] and D. J. Henderson[3]
[1]Cyclone Testing Station, James Cook University, Townsville, Mitchell.Humphreys@my.jcu.edu.au
[2]Cyclone Testing Station, James Cook University, Townsville, John.Ginger@jcu.edu.au
[3]Cyclone Testing Station, James Cook University, Townsville, David.Henderson@jcu.edu.au

ABSTRACT

Air-leakage tests on the nominally sealed JCU-ASI Shed showed that the porosity ranges from about 0.5% to 1.4% on the walls. The mean internal pressure in these types of buildings can be estimated analytically given the areas and distribution of openings and the corresponding mean external pressures on the envelope. The internal pressure fluctuations in these types of buildings with a large opening are attenuated relative to the external pressures due to added damping from the porosity.

1. Introduction

Design internal pressures on a building specified in standards (i.e. AS/NZS 1170.2 (2011)) depends on the openings and the porosity in the envelope. The internal pressure in a nominally sealed building is generally lower than the external pressures. However, a large opening can generate large internal pressures in strong winds, and in combination with large external pressures can result in large net pressures across the envelope. Recent studies by Humphreys (2020) summarized in this paper quantifies the porosity (background leakage) in the envelope of a typical Shed enables the internal pressures to be calculated reliably and the structural design of these types of buildings to be optimised.

1.1 JCU-ASI Shed

The 6 × 6 × 3 m James Cook University – Australian Steel Institute Shed (JCU-ASIS) is a cold-form, portal-framed building with typical construction details and tolerances with an 11° roof pitch and a nominal internal volume (V_B) of 119 m^3, shown in Figure 1a, was used in a series of tests as described by Humphreys (2020). Figure 1b shows the schematic layout of the JCU-ASIS, its fitments including two roller doors, three sliding windows, and a personal access door, and the location of pressure taps.

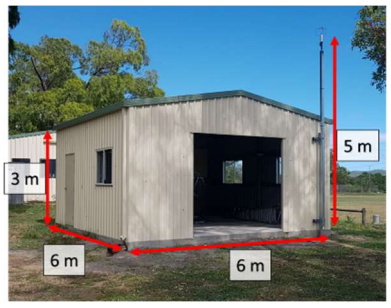

(a)

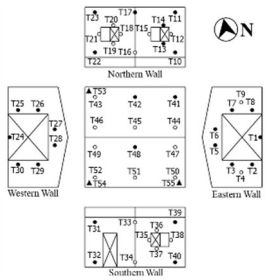

(b)

Fig 1. a) JCU-ASIS with roller door open on East Wall. Anemometer attached to 5 m mast at NE edge. b) Schematic of JCU-ASIS wall fitments and pressure tap layout; o – external taps; ▲ – internal taps

2. Porosity and flexibility of the envelope, and air leakage testing

The porosity of a building envelope depends on the gaps around fitments, construction tolerances and installation and construction practices. Humphreys (2020) determined the porosity by pumping air into the building to induce a steady differential pressure $\Delta\bar{p}$ across the envelope and measuring the steady-state air flow-rate, $\bar{Q}$ required across the building envelope. The porous opening area A_p is found using Equation 1, by applying the discharge coefficient, k = 0.61 and density of air ρ = 1.2 kg/m^3.

$$\bar{Q} = kA_P\sqrt{2|\Delta\bar{p}|/\rho} \quad (1)$$

The flow through openings are also described by the power-law given by $\bar{Q} = C(\Delta\bar{p})^n$, where the empirical flow coefficient C and flow-exponent n are derived by Humphreys (2020). The initial "baseline" air-leakage test was carried out by sealing gaps (porous openings) as much as practicable, as described by Humphreys (2020) (Stage 1). Further air-leakage tests were carried out by progressively removing the seals from selected parts of the envelope and repeated until all porous openings were unsealed and tested (Stage 9). The air pumped into the building during air-leakage tests is expressed as flow-rate per unit wall area, as an effective measure of permeability relative to the pressure drop across the envelope. Figure 2 shows the air-leakage test flow-rate $(\bar{Q})$ per unit wall area versus differential pressure across the envelope $(\Delta\bar{p})$, for Stage 1 (Baseline Building) and Stage 9 (Nominally sealed + sealed Eastern roller-door), the TTU WERFL building (Yeatts, 1994), a typical Australian house tested by the CSIRO (Michell and Biggs, 1982), and averaged results from several supermarkets, schools, and high-rise buildings (Shaw and Jones, 1979). Figure 2 shows that the effective permeability of the Baseline JCU-ASIS (Stage 1) is similar to the Australian house and a High Rise building. The Nominally sealed JCU-ASIS + sealed East roller door (Stage 9) (i.e. typical industrial building in tropical climates) is considerably more porous than all other building types. Humphreys (2020) showed the porous opening areas, A_p derived from each sequential air-leakage test using the Power-law coefficients and the steady discharge Equation 1 were very similar, as the empirical flow exponent n is about 0.5. He also determined the background leakage around the wall fitments (per unit) and general construction gaps (per meter length). This data is used to define the area of background leakage in each wall of the JCU-ASIS. The porosity of the JCU-ASI Shed $\varepsilon = A_p/A_T$ is about 1 %.

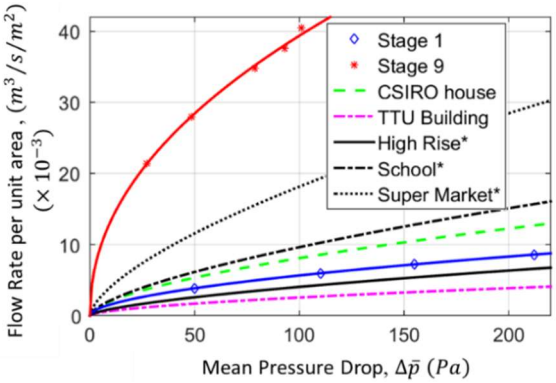

Fig 2. Mean flow rate per unit wall area vs mean pressure drop across the envelope of JCU-ASIS compared with other buildings tested

The flexibility of a building envelope will influence the internal pressure fluctuations and is accounted for by increasing the building volume, such that the effective building volume $V = V_B(1 + K_A/K_B)$, where V_B is the nominal building volume = 119 m^3. Here, the bulk modulus of the building $K_B = \Delta p/(\Delta V/V)$, is the change in the internal pressure per unit volumetric strain and $K_A =$ the bulk modulus of air. Humphreys (2020) carried out a series of tests and showed that K_A/K_B is about 3 for the JCU-ASIS and therefore $V = 119 \times (1 + 3) = 476$ m^3.

3. Wind induced pressures

Humphreys (2020) studied the wind-induced internal pressures in the JCU-ASI Shed in two parts: (i) with a nominally sealed envelope (ii) with a range of window and roller-door openings. The wind speed and directions, and corresponding external and internal pressures on the JCU-ASI Shed, were analysed. The distribution of porosity from the air-leakage testing is also used for determining the open areas in the envelope. Most of the data obtained was for the nominally sealed JCU-ASIS. Mean approach wind angles within ±30° from the orthogonal building axes were used to define the windward wall.

3.1 Nominally sealed building

External and internal pressures were measured on the nominally sealed JCU-ASI Shed with all the doors and windows closed and the top and bottom of the West roller door sealed, defined by Humphreys (2020) as Case NS2. This case has a porosity distribution similar to a building with a single roller door on the East Wall. The porosity of the roof is negligible compared to the walls. Figure 3a shows the spatially-averaged external pressure on the four walls and the internal pressure for Case NS2. The wall pressures were acquired from averaging of pressures on Taps; East: T1, T2, T3, T5, T6, T7 and T8; North: T10, T11, T17, T22 and T23; West: T24, T25, T26, T27, T28, T29 and T30; and South: T31, T32, T39, and T40. Figure 3a shows that the internal pressure is mostly influenced by the windward East wall pressure (most porous wall of the JCU-ASIS with a ≈ 35mm gap above the roller-door). Figure 3b shows the spatially-averaged external wall pressure spectra and internal pressure spectrum for Case NS2. The windward East wall pressure fluctuations are similar to the wind velocity fluctuations with most of the energy below 0.5 Hz. The leeward West wall in the wake of the building has the least amount of pressure energy. The internal pressure fluctuations are significantly attenuated compared to the windward and sidewall pressure fluctuations. The pressure fluctuations admitted through the envelope that generate the internal pressure fluctuations, is described by Vickery (1986) as the characteristic frequency f_c =0.6 Hz for building Case NS2.

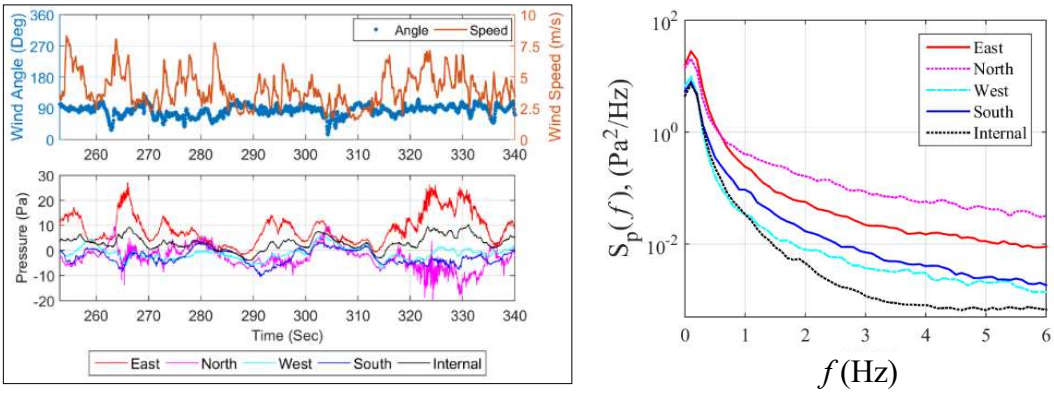

(a) (b)

Fig 3. a) Wind speed, wind direction, and internal and area-averaged external pressures vs time,
b) Internal and area-averaged external wall pressure spectra: Case NS2, $\bar{\theta} \cong 90°$

3.2 Building with a Large Windward Wall Opening

Humphreys (2020) conducted tests with either the window open on the North Wall (Case #1) or the roller-door open on the East Wall (Case #5). All large opening tests were conducted with seals above and below the West roller-door (as in Case NS2). The A_w/A_L ratio for Case #1 is 1.06 and for Case #5 is 19.9. Here A_w is the windward wall open area and all other wall open areas are combined into A_L. When $A_w/A_L \geq 2$, the mean external pressure at the windward opening contributes about 80% to the mean internal pressure and the opening is considered dominant in AS/NZS1170.2 (2011).

Typical time histories of wind speed, approach wind angle, and internal and external pressures for Cases #1 and #5 are shown in Figures 4a and 4b respectively. Here the external pressures from near the large openings are, tap T13 above the North window for Case #1, and tap T7 beside the East roller door for Case #5. Figures 4a and 4b show that for the larger opening Case #5, where A_W/A_L is about 20, the mean internal pressures is similar to the external pressure at tap T7 beside the large opening, and the internal pressure fluctuations are significantly attenuated for Case #1.

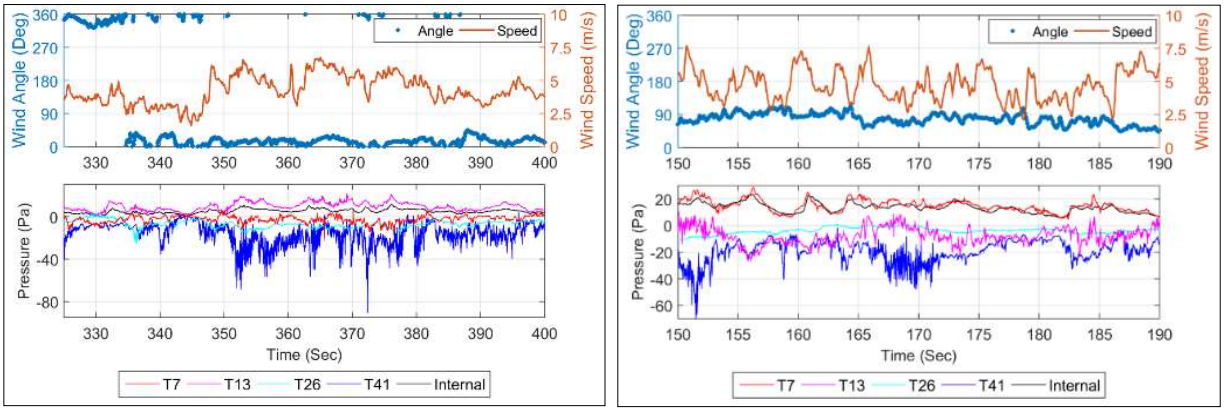

a) Case #1, $\bar{\theta} \cong 0°$ b) Case #5, $\bar{\theta} \cong 90°$

Fig 4. Wind speed, wind direction and internal and external point pressures vs time

Figures 5a and 5b show the effective area-averaged external pressure spectra on the openings for Cases #1 and #5, and the internal pressure spectra. Figure 5a shows the internal pressure fluctuations for Case #1 ($A_w/A_L \approx 1.1$) are damped compared to the area-averaged pressure on the window. Figure 5b (i.e. Case #5) shows that the internal pressure spectrum is equal to the external pressure up 1 Hz, with attenuation increasing beyond 1 Hz. Figures 5b also show that the internal pressure fluctuations near the Helmholtz frequency $f_H = [(a_s/2\pi)\sqrt{(\sqrt{A}/(C_I V))}$ = 3.4 Hz calculated with C_I = 1.4, A = 6.6m^2, speed of sound a_s = 340 m/s and $V = 119 \times (1 + 3)$ = 476 m^3, is highly damped.

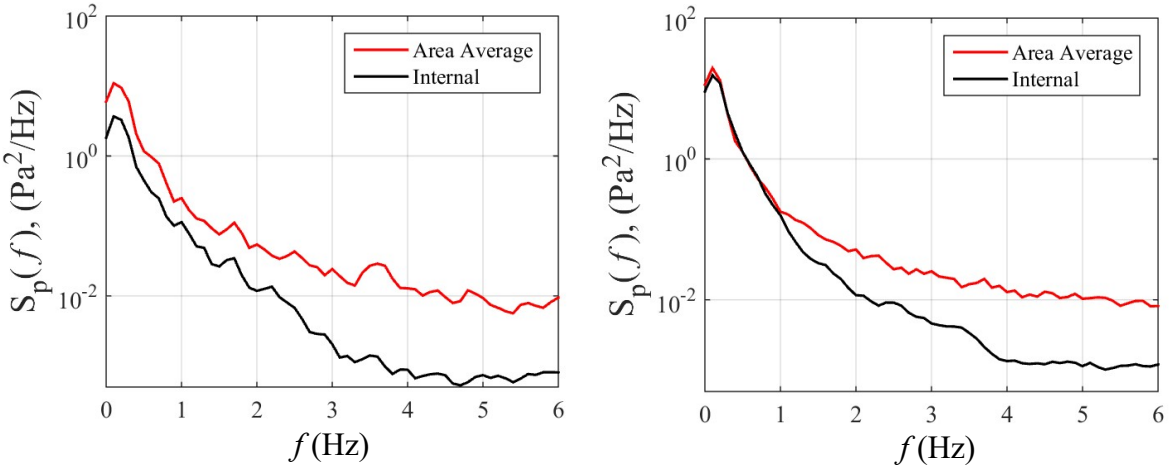

a) Case #1, $\bar{\theta} \cong 0°$ b) Case #5, $\bar{\theta} \cong 90°$

Fig 5. Pressure spectra of internal and effective area-averaged external pressure on opening

3.3 Internal to External Pressure Ratios

The mean internal pressure $\bar{p}_i$ can be derived analytically using Equation 2, where mean pressures and the corresponding open areas on the windward and leeward areas A_W and A_L are known for nominally sealed and buildings with large openings in the envelope.

$$\bar{p}_i = \bar{p}_{e,w} \Big/ \left(1 + \left(\frac{A_L}{A_w}\right)^2\right) + \bar{p}_{e,L} \Big/ \left(1 + \left(\frac{A_W}{A_L}\right)^2\right) \quad (2)$$

Humphreys (2020) found that the ratio $\left([\bar{p}_i - \bar{p}_{e,L}]/[\bar{p}_{e,w} - \bar{p}_{e,L}]\right)$ calculated from the experimental data is equal to that obtained analytically using Equation 2, as shown in Figure 6. The mean internal pressures can be estimated satisfactorily as a function of the windward and leeward opening area ratio from Equation 2. The windward and leeward wall mean external pressures were estimated by averaging the pressures across the windward wall and the leeward walls for the nominally sealed cases, and around the large windward wall opening and the leeward walls for the large opening cases. These findings are similar to results by Ginger (2000) for the full-scale TTU WERFL building.

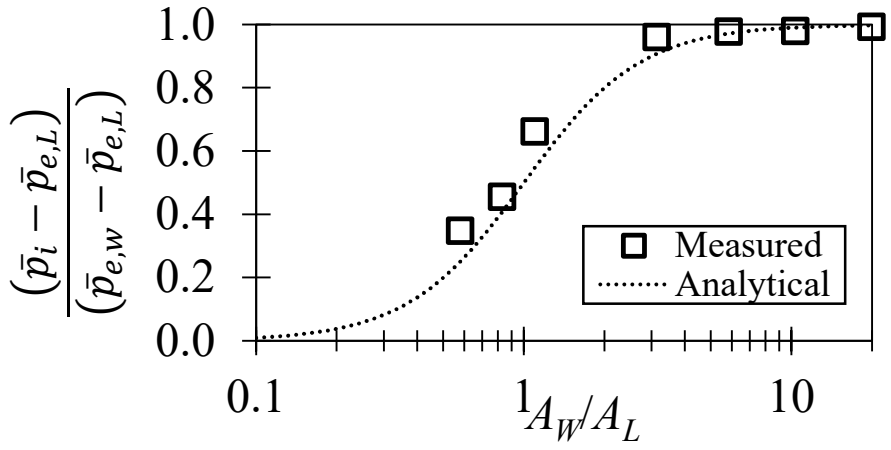

Fig 6. Measured and analytical mean internal pressure relative to mean external Windward and Leeward wall pressure differential vs A_w/A_L

The nominally sealed building tests NS1 and NS2 with A_w/A_L of 0.58 and 0.83 respectively, and the building with the large opening Case #1 (A_w/A_L of 1.06), estimated slightly lower internal pressures possibly because of the uneven background leakage distribution that is not accurately accounted for in the simplified analytical calculation. The measured mean internal pressures closely match the analytical values obtained from Equation 2, when $A_w/A_L > 3$ (Cases #2 to #5) in tests by Humphreys (2020). Equation 2 provides a good estimate for deriving the quasi-steady internal pressure, $\bar{p}_i$ when $\bar{p}_{e,w}$, $\bar{p}_{e,L}$ and A_w/A_L are known, especially for a large windward openings (i.e. $A_W/A_L \geq 10$).

AS/NZS 1170.2 (2011) defines peak (i.e. design $\hat{p}$ or $\check{p}$) internal and external pressures with respect to a 0.2-second peak design wind speed $\hat{U}_h$ (at mid-roof-height), where $\hat{p}$ (or $\check{p}$) = $\tilde{C}_p ½ \rho \hat{U}_h^2$. Here, the quasi-steady approximation infers that pressure fluctuations follow the approach wind velocity fluctuations and that the ratio of the peak to mean pressure (peak pressure factor $G_p = \hat{p} / \bar{p}$) = $\left(\hat{U}_h/\bar{U}_h\right)^2$. Further, AS/NZS 1170.2 (2011) apples the quasi-steady methodology $\hat{p}_i = G_{pi} \times \bar{p}_i$, where $\bar{p}_i$ is a function of A_w/A_L. Humphreys (2020) found that the G_{pi}, $G_{pe,w}$, Cases #1 to #5, are about 2.5. This is similar to the quasi-steady gust factor (i.e. velocity gust factor squared) in AS/NZS 1170.2 (2011) for Terrain Category 2 at a 5 m height of $2.95 = 1.72^2$. However, the pressure factor for internal pressures for the nominally sealed cases NS1 and NS2 are significantly lower.

4. Conclusions

A full-scale study was conducted on the James Cook University – Australian Steel Institute Shed (JCU-ASIS) by Humphreys (2020) to determine the wind-induced internal pressure fluctuations. Air-leakage tests were carried out to determine the distribution of porosity (background leakage) of the building envelope. Measurements were carried out on the Nominally sealed JCU-ASIS (Cases NS1 and NS2) and JCU-ASIS with a large windward wall opening (Cases #1 to #5). The results provide unique full-scale internal pressure data to assess the internal pressure response in a typical Shed with respect to analytical methods and other studies. A summary of tests and results are presented in this paper.

The air-leakage tests provide the magnitude and distribution of porosity around the envelope. The results show the porosity of the nominally sealed JCU-ASIS walls range from about 0.5% to 1.4% depending on the number and type (window, roller-door) of wall fitments. This porosity is higher than other building types, especially those built in cooler climates. The deformation of the JCU-ASIS envelope was measured and the effective volume was determined to be about 4 times the nominal building volume, equal to about 476 m^3.

The mean internal pressure in these types of buildings can be estimated analytically if the areas and distribution of openings on the envelope and the corresponding mean external pressures are known. The internal pressure fluctuations in the nominally sealed JCU-ASIS are small compared to external pressures, and increase as the windward to leeward opening area increases.

The internal pressure fluctuations in these types of buildings with a large windward wall opening are attenuated relative to the external pressures applied to the opening due to added damping from the porosity. The porosity (background leakage) also significantly damps Helmholtz resonance.

Acknowledgements

The authors acknowledge the support of the Australian Research Council Linkage Grant and the Australian Steel Institute – Shed Group (Industry Partner) to conduct this research.

References

Standards Australia, (2011), "Structural design actions. Part 2 Wind actions", Australian/New Zealand Standard, AS/NZS 1170.2:2011.

Ginger, J. D., (2000.), “Internal pressure and cladding net wind loads on full scale low-rise building”, ASCE J. Structural Engineering Vol 126 Part IV 538-543.

Humphreys, M. T., (2020), “Characteristics of Wind-Induced Internal Pressures in Industrial Buildings with Wall Openings”, PhD Thesis, James Cook University, Australia.

Vickery, B. J., (1986), “Gust-Factors for Internal-Pressures in Low Rise Buildings”. *Journal of Wind Engineering and Industrial Aerodynamics, 23*(1-3), 259-271. doi:10.1016/0167-6105(86)90047-4

Michell, D. and Biggs, K. L. (1982), “An Apparatus for air-tightness measurements on houses” Revision of Building Research: BUILDING RESEARCH Melb

Yeatts, B. B., (1994), “ Internal Pressure For Buildings”. (Master of Science), Texas Tech University

Shaw, C. Y. and Jones, L., (1979), “Air tightness and air infiltration of school buildings” ASHRAE Transactions, 85(1), 85 - 95.